

Mechanism of Inactivation of γ -Aminobutyric Acid Aminotransferase by (1*S*,3*S*)-3-Amino-4-difluoromethylene-1-cyclopentanoic Acid (CPP-115)

Hyunbeom Lee,^{†,⊥} Emma H. Doud,^{†,‡} Rui Wu,[§] Ruslan Sanishvili,^{||} Jose I. Juncosa,^{†,¶} Dali Liu,[§] Neil L. Kelleher,^{†,‡} and Richard B. Silverman^{*,†,‡}

[†]Department of Chemistry, Chemistry of Life Processes Institute, and Center for Molecular Innovation and Drug Discovery, Northwestern University, 2145 Sheridan Road, Evanston, Illinois 60208-3113, United States

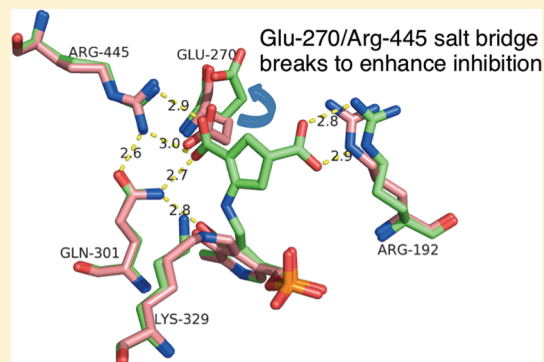
[‡]Department of Molecular Biosciences, Northwestern University, Evanston, Illinois 60208, United States

[§]Department of Chemistry and Biochemistry, Loyola University Chicago, 1068 W. Sheridan Road, Chicago, Illinois 60660, United States

^{||}X-ray Science Division, Argonne National Laboratory, Argonne, Illinois 60439, United States

Supporting Information

ABSTRACT: γ -Aminobutyric acid aminotransferase (GABA-AT) is a pyridoxal 5'-phosphate (PLP)-dependent enzyme that degrades GABA, the principal inhibitory neurotransmitter in mammalian cells. When the concentration of GABA falls below a threshold level, convulsions can occur. Inhibition of GABA-AT raises GABA levels in the brain, which can terminate seizures as well as have potential therapeutic applications in treating other neurological disorders, including drug addiction. Among the analogues that we previously developed, (1*S*,3*S*)-3-amino-4-difluoromethylene-1-cyclopentanoic acid (CPP-115) showed 187 times greater potency than that of vigabatrin, a known inactivator of GABA-AT and approved drug (Sabril) for the treatment of infantile spasms and refractory adult epilepsy. Recently, CPP-115 was shown to have no adverse effects in a Phase I clinical trial. Here we report a novel inactivation mechanism for CPP-115, a mechanism-based inactivator that undergoes GABA-AT-catalyzed hydrolysis of the difluoromethylene group to a carboxylic acid with concomitant loss of two fluoride ions and coenzyme conversion to pyridoxamine 5'-phosphate (PMP). The partition ratio for CPP-115 with GABA-AT is about 2000, releasing cyclopentanone-2,4-dicarboxylate (**22**) and two other precursors of this compound (**20** and **21**). Time-dependent inactivation occurs by a conformational change induced by the formation of the aldimine of 4-aminocyclopentane-1,3-dicarboxylic acid and PMP (**20**), which disrupts an electrostatic interaction between Glu270 and Arg445 to form an electrostatic interaction between Arg445 and the newly formed carboxylate produced by hydrolysis of the difluoromethylene group in CPP-115, resulting in a noncovalent, tightly bound complex. This represents a novel mechanism for inactivation of GABA-AT and a new approach for the design of mechanism-based inactivators in general.



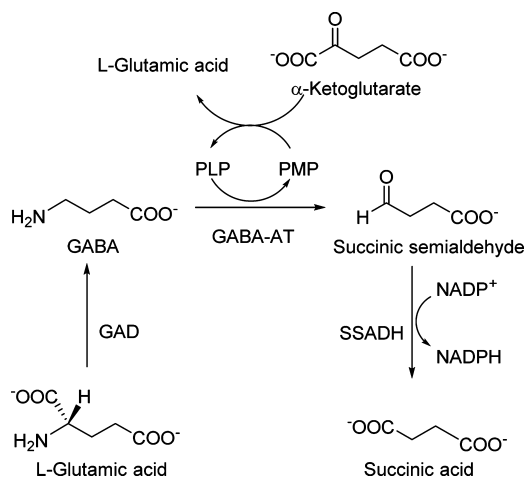
INTRODUCTION

γ -Aminobutyric acid (GABA) is a major inhibitory neurotransmitter in the mammalian central nervous system.¹ When GABA concentrations in the brain fall below a threshold level, convulsions occur.² It has also been found that Alzheimer's disease,³ Huntington's chorea,⁴ Parkinson's disease,^{5,6} and drug addiction^{7,8} are related to diminished GABA levels in the brain. GABA is produced by the α -decarboxylation of the excitatory neurotransmitter L-glutamic acid, catalyzed by the pyridoxal 5'-phosphate (PLP)-dependent enzyme glutamic acid decarboxylase (GAD, Scheme 1). GABA is metabolized by γ -aminobutyric acid aminotransferase (GABA-AT), also a PLP-dependent enzyme, to succinic semialdehyde, which is further oxidized to succinic acid by succinic semialdehyde dehydrogen-

ase (SSDH). Degradation of GABA to succinic semialdehyde converts the PLP coenzyme to pyridoxamine 5'-phosphate (PMP); α -ketoglutarate is used in a second step to return PMP to PLP with concomitant formation of L-glutamic acid. Therefore, the concentrations of the inhibitory (GABA) and excitatory (L-Glu) neurotransmitters are regulated by the appropriate balance between GAD and GABA-AT.⁹

When GABA is injected directly into the brain of a convulsing animal, the seizures are terminated.¹¹ However, because GABA does not cross the blood-brain barrier, peripheral GABA administration is not an effective approach

Received: December 2, 2014

Scheme 1. GABA Metabolism¹⁰

for the treatment of epilepsy. An alternative approach to increase GABA levels in the brain is by inhibition of GABA-AT, which blocks the degradation of GABA.¹² A mechanism-based inactivator, an unreactive compound that initially acts as a substrate for the target enzyme and is converted to a species that causes inactivation of that enzyme, generally by covalent attachment, could increase GABA levels for an extended period of time.¹³ The design of these types of inhibitors requires insight into the mechanism of the target enzyme so that the catalytic chemistry can be utilized in the activation of the inactivator; the mechanism of the first half of the “ping-pong” reaction catalyzed by GABA-AT is shown in Scheme 2.

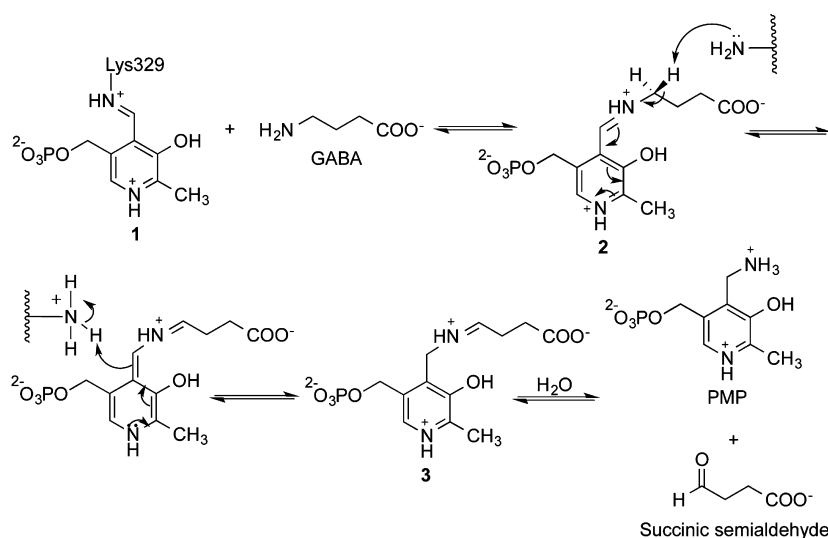
Incubation of GABA with GABA-AT leads to the conversion of a lysine-PLP aldimine (**1**) to a GABA-PLP aldimine (**2**). Abstraction of the γ -proton by Lys329 and tautomerization leads to a PMP aldimine (**3**); enzyme-catalyzed hydrolysis of this intermediate leads to succinic semialdehyde and PMP.¹⁴

4-Amino-5-hexenoic acid (**4**, γ -vinyl-GABA; vigabatrin) is a mechanism-based inactivator of GABA-AT¹⁵ that is an FDA-approved drug (Sabril) to treat infantile spasms and refractory partial seizures. However, because of a serious side effect, namely, retinal damage and blindness, a drug with more potency and less toxicity was desired. Mechanistic studies

performed by Nanavati and Silverman¹⁶ (Scheme 3) demonstrated that vigabatrin inactivates GABA-AT via two mechanisms, a Michael addition reaction and an enamine reaction, in a ratio of 70:30. In the Michael addition pathway (pathway a), vigabatrin acts like substrate GABA and undergoes aldimine formation with PLP, deprotonation, and tautomerization to a Michael acceptor (**5**), which undergoes Michael addition by Lys329, the lysine residue to which PLP is bound in the native enzyme,¹⁷ giving, after protonation, covalent adduct **6**. Enzyme-catalyzed hydrolysis of **5** gives α,β -unsaturated ketone **7**, which may be a possible cause for side effects of the drug. In the enamine pathway (pathway b), an enamine intermediate (**8**), formed by tautomerization through the alkene, attacks the enzyme-bound PLP to inactivate GABA-AT (**9**), also by formation of a covalent adduct. Hydrolysis of **8** gives a weak electrophile, which is unlikely to proceed through further reactions in the active site.

To avoid the potentially toxic intermediate (**7**), computer modeling based on the crystal structures of GABA-AT¹⁸ and the vigabatrin-PLP complex in GABA-AT¹⁷ was carried out to determine how to prevent the Michael addition pathway. The model predicted that, in the energy-minimized structure, the alkene double bond pointed away from the nucleophilic Lys329; for Michael addition to occur, that bond had to rotate, allowing the alkene to be aligned with the side chain amine of Lys329. A conformationally rigid vigabatrin analogue was prepared (**10**) to prevent Michael addition, and it was found that it inactivated GABA-AT exclusively by the enamine pathway;¹⁹ however, it was a weak inactivator. The second approach to prevent formation of reactive product **7** was to synthesize a vigabatrin analogue that would give rapid Michael addition so that the equivalent of intermediate **5** would not be sufficiently stable to allow the enzyme-catalyzed hydrolysis leading to the equivalent of **7**.²⁰ That approach required the synthesis of a compound with the alkene pointing toward the side chain amine of Lys329 (**11**). The obtained compound inactivated GABA-AT, but only in the absence of the electrophilic trapping agent 2-mercaptoethanol. Therefore, an undesirable reactive intermediate (the corresponding ketoacid of **11**) was formed prior to inactivation. To accelerate the inactivation rate, two electron-withdrawing fluorine atoms were

Scheme 2. First Catalytic Reaction of GABA-AT



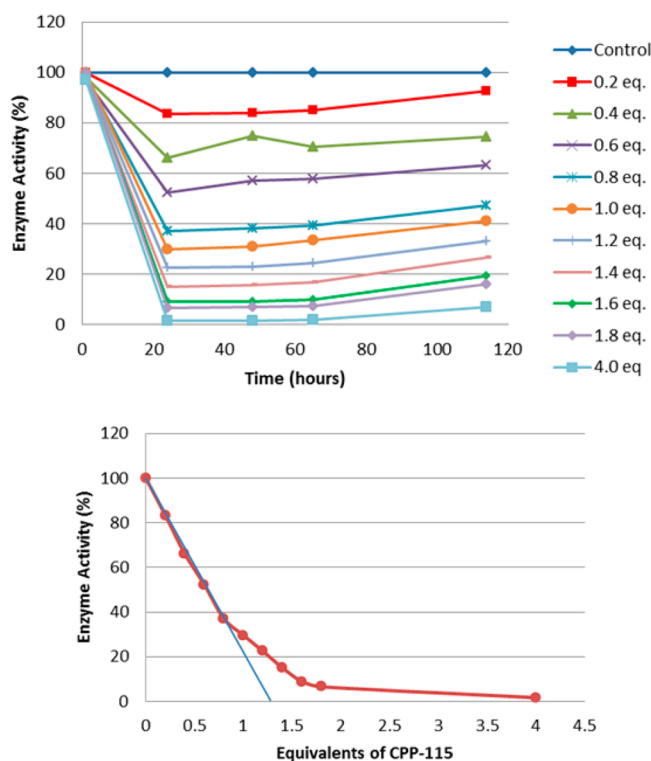


Figure 1. (Top) Time-dependent inactivation of GABA-AT by 0–4.0 equiv of CPP-115. (Bottom) Determination of the turnover number for the inactivation of GABA-AT by CPP-115. The data points at 24 h are replotted as enzyme activity vs equiv of CPP-115.

the activity of the enzyme returned to about 8%; with 2000 equiv of CPP-115, the activity return was only 1%, even after 50 h of dialysis.

Fluoride Ion Release during Inactivation of GABA-AT by 2 mM CPP-115. Upon incubation of GABA-AT with CPP-115, fluoride ions were continually released, even after the enzyme's activity had fallen to almost zero (Figure S3, Supporting Information). After normalization of the values with the controls, it was found that 66 ± 3 equiv of fluoride ions were released slowly over a period of 27 h. However, when the same experiment was repeated with PLP supplemented in the mixture, there were 127 ± 5 equiv of fluoride ions released over time. Because α -ketoglutarate is essential to regenerate PLP from PMP, if α -ketoglutarate is omitted, the amount of fluoride ions released per single turnover of inhibition can be determined. The continual release of fluoride ions was not observed when there was no α -ketoglutarate present, and only 4.3 ± 0.5 equiv of fluoride ions were detected per enzyme dimer (Figure S4, Supporting Information). However, when α -ketoglutarate was added to the inactive enzyme, even without supplementation with PLP, the fluoride ion concentration began to increase. A control experiment with no enzyme in the incubation mixture was performed, which confirmed that no fluoride ions were released from CPP-115 in the absence of the enzyme, even if PLP is added.

Inactivation of [^3H]PLP-Reconstituted GABA-AT by CPP-115. To determine the fate of the coenzyme by inactivation with CPP-115, apo-GABA-AT was reconstituted with [^3H]PLP. The maximum recovered activity was 71.4% of the original, and the activity recovery plateaued after 5 h of the reactivation process (Table 1), indicating that 29.6% of the enzyme remained inactive.

Table 1. Return of GABA-AT Activity after apo-GABA-AT Was Incubated with [^3H]PLP

	2 h	3 h	4 h	5 h	original
dA ($\text{mL}^{-1} \text{min}^{-1}$)	0.630	0.748	1.504	1.522	2.124

[^3H]PLP-GABA-AT was inactivated with CPP-115, and the released radioactive compounds were analyzed using HPLC (Figure S5, Supporting Information). The experiment was performed with two controls: CPP-115 was omitted in a negative control (all radioactivity should be labeled PLP), and GABA replaced CPP-115 with α -ketoglutarate omitted in a positive control (all radioactivity should be PMP). The negative control released most of its radioactivity as PLP (but none as PMP), whereas a GABA-incubated control released both PMP and PLP (Figure S6, Supporting Information). Given that the positive control with GABA should only produce PMP from active enzyme, the PLP present in this sample represents that released from the inactive portion of GABA-AT. After the background radioactivity from the control experiments was subtracted from the CPP-115 experiment, CPP-115-inactivated [^3H]PLP-reconstituted GABA aminotransferase was found to release 100% of its cofactor as [^3H]PMP (Figure S7, Supporting Information). The small radioactive peak at 33 min was confirmed to be degraded PLP present in all of the samples.

Mass Spectrometric Analysis of Metabolites from Inactivation of GABA-AT with CPP-115. Metabolites released during inactivation were determined by LC/MS/MS. After inactivation of GABA-AT by CPP-115 followed by denaturation and filtration, three metabolites were identified from the sample solution that were not present in the control samples: [m/z] 127.0389, 171.0291, and 401.0745 (A, B, and C in Figure S8, Supporting Information, respectively), corresponding to 22, 21, and 20, respectively, in Scheme 5 (see Discussion). These parent ions were selected for fragmentation using normalized collision energies. Fragmentation data for m/z 127.0389 (Supporting Information Figure S9) confirmed the structure of 3-oxo-1-cyclopentanecarboxylic acid (22). MS/MS for m/z 171.0291 and 401.0745 (Supporting Information Figures S10 and S11, respectively) confirmed the structures of 21 and 20.

Intact Mass Spectrometry of GABA-AT. Since covalent modification of GABA-AT was not detected using middle down proteomics (see Figures S12–S14 in Supporting Information), we analyzed the intact GABA-AT protein to see if any detectable mass shifts were present. The intact mass data showed multiple peaks, indicating that the GABA-AT purified from pig brain was a mixture of GABA-AT species with different N-termini. Three samples were tested using LC/MS/MS: free enzyme (negative control), vigabatrin-inactivated GABA-AT (positive control), and CPP-115-inactivated GABA-AT (Figure S15, Supporting Information). Vigabatrin-inactivated GABA-AT showed an added mass of 122 Da from the mass of the native enzyme, which matches the covalent adduct proposed previously.¹⁵ However, CPP-115-inactivated GABA-AT showed no significant peaks corresponding to any added mass. To stabilize any potential imine adducts throughout the LC/MS/MS process, the samples were reduced with sodium borohydride as described previously for crystallography studies. Reduction resulted in stabilization of the PLP cofactor on the enzyme, with an added mass of 236 from the original peak (M). As expected, the peaks of vigabatrin-inactivated GABA-AT

(Figure S16, Supporting Information) were no different from those in Figure S15 since the vigabatrin covalent adduct is stable.¹⁵ Interestingly, for CPP-115-inactivated GABA-AT, reduction had no effect on the resulting data and showed no added mass on the protein.

X-ray Crystallography of Native and CPP-115-Inactivated GABA-AT. To understand how time-dependent inactivation of GABA-AT by CPP-115 could occur without covalent modification of the protein or cofactor, CPP-115-inactivated and dialyzed GABA-AT were crystallized. The crystal structures of native GABA-AT from pig brain and inactivated enzyme were obtained at 1.63 Å and 2.19 Å resolution, respectively. The crystal structure for the native pig brain enzyme was very similar to that reported from pig liver by Storici et al.¹⁸ The crystal structures of the native enzyme and the inactivated enzyme were compared to analyze the difference in overall structure (Figure 2) and in the active site (Figure 3).

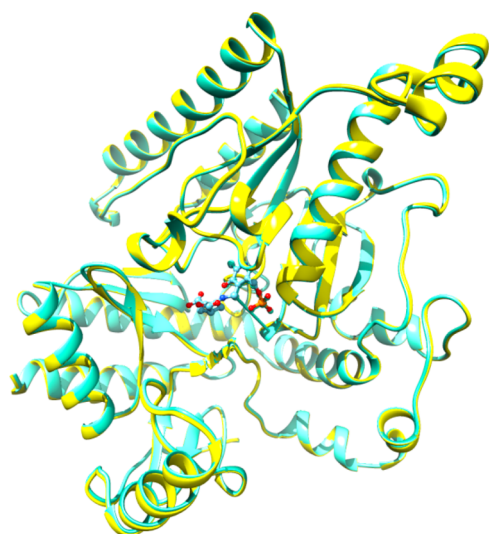


Figure 2. Ribbon diagram of the superimposed native GABA-AT (yellow) and GABA-AT (cyan) bound to CPP-115.

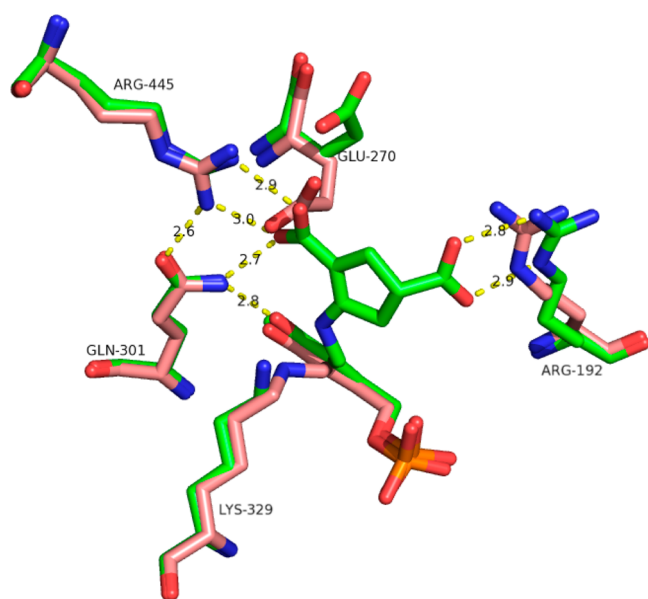


Figure 3. Superimposition of the crystal structures of native GABA-AT (pink) and CPP-115-inactivated GABA-AT (green).

The active site of the inactivated GABA-AT was investigated to understand the ligand–enzyme interactions (Figure 4); the omit map supports the ligand interpretation (see Supporting Information, Figure S17).

DISCUSSION

At the start of this investigation, we considered a variety of likely mechanisms for the inactivation of GABA-AT by CPP-115 (Schemes 4–8)^{23,24} and then considered experiments to differentiate them. All of these inactivation mechanisms are initiated by the same steps shown in Scheme 2 for substrate turnover or the two inactivation mechanisms for vigabatrin shown in Scheme 3. In mechanism 1 (Scheme 4), following γ -proton abstraction of **13**, tautomerization leads to an α,β -unsaturated intermediate (**14**), which is attacked by the active site lysine residue or another base to covalently modify the enzyme. No fluoride is released, the enzyme is inactivated, and hydrolysis of **15** gives **16** with release of PMP as the cofactor.

If intermediate **15** in Scheme 4 (where X is either the active site lysine residue or OH from attack by water) eliminates one fluoride ion (Scheme 5), the inactivator can form another reactive α,β -unsaturated imine (**17**), which can be attacked by a water molecule to release the other fluoride ion, forming **18**. Depending on what X is, this may result in inactivation or turnover. If X is the active-site lysine residue (**15a**, pathway a, Scheme 5), the intermediate is a stabilized amide; hydrolysis generates covalent adduct **19** with the release of PMP. However, if X is a hydroxyl group (**15b**, pathway b, Scheme 5) formed by water molecule attack on reactive intermediate **14** (Scheme 4), stable dicarboxylate intermediate **20** will form; hydrolysis gives metabolite **21** and PMP, and subsequent decarboxylation of **21** gives **22**.

The third potential mechanism involves allylic tautomerization of external aldimine **13** to form **23** (Scheme 6). Because **23** also is a reactive electrophile, it may undergo Michael addition to form adduct **24**, which could be hydrolyzed to give **25** and release PMP.

In the fourth potential mechanism (Scheme 7), intermediate **23** (Scheme 6) can proceed through three different pathways. Pathway a generates an enamine (**26**), similar to that formed during vigabatrin inactivation; this species might undergo enamine attack on the Lys329-bound PLP to form covalent adduct **27**, which could hydrolyze to **28**. In pathway b, one fluoride ion is released by nucleophilic substitution (**29**) before undergoing transimination to form enamine adduct **30**, which might undergo hydrolysis to **31**. Pathway c from **30** involves elimination of a second fluoride ion (**32**) followed by hydrolysis to give **33**.

The final potential mechanism involves fluoride ion elimination from enamine **26** to generate reactive Michael acceptor **34** (Scheme 8). Hydrolysis of imine **34** (pathway a) gives **35** and PLP. Attack by an active site nucleophile (either Lys329 or water; pathway b) gives either covalent adduct **36** or noncovalent adduct **37**, respectively. Elimination of another fluoride ion forms **38** or **40**, each of which can be subsequently hydrolyzed to covalent adduct **39** or metabolite **41**; further hydrolysis of **39** would also give **41**. In either case, this mechanism releases the cofactor as PLP. All of these possible mechanisms can be differentiated by determination of the number of fluoride ions released, the fate of the cofactor, and the final metabolites or adducts formed; these possibilities are summarized in Table 2.

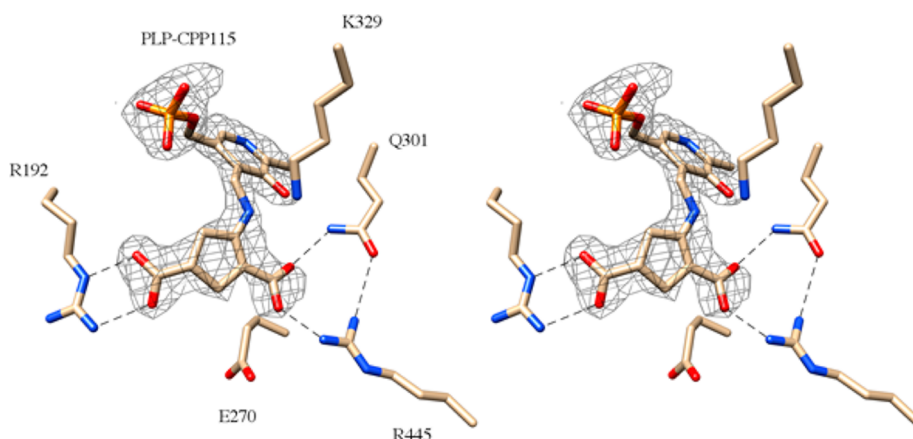
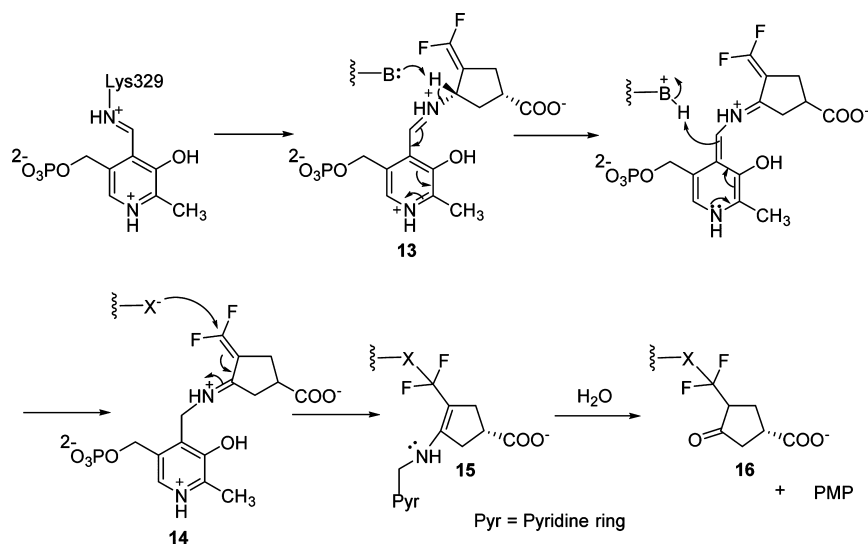


Figure 4. Stereoview of GABA bound by the CPP-115 adduct. The $2F_o - F_c$ electron-density map is shown as light gray mesh at 1.1σ level around the CPP-115 adduct.

Scheme 4. First Potential Mechanism of Inactivation of GABA-AT by CPP-115



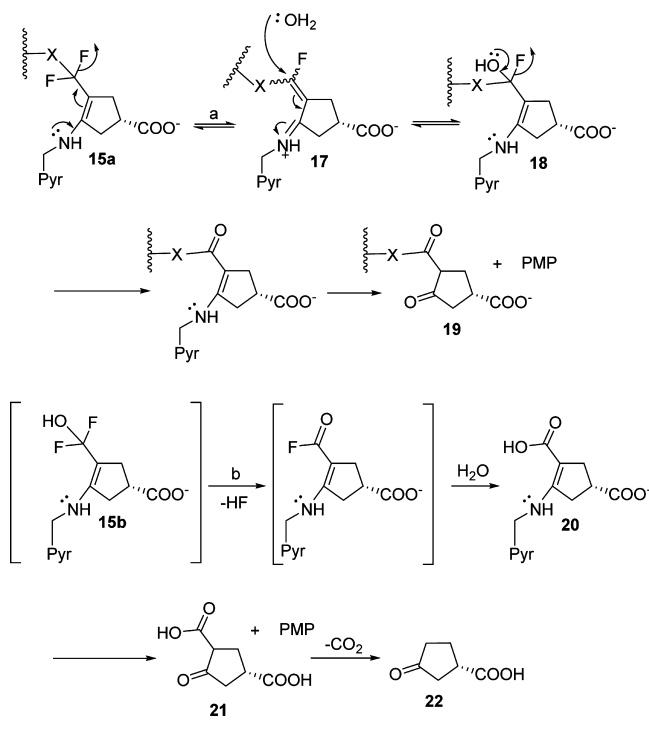
The partition ratio, the number of inactivator turnovers per inactivation event, was investigated by determination of the number of molecules of CPP-115 that were required to cause complete enzyme inactivation. Time-dependent inhibition was observed for 1–4 equiv of CPP-115, although pseudo-first-order kinetics was not observed (Figure 1, top). A replot of these data with extrapolation of the first few data points gave a turnover number of 1.3 ± 0.3 per active site (Figure 1, bottom). The nonpseudo-first-order inactivation kinetics displayed indicated possible product inhibition and suggested possibly two concurrent mechanisms occurring at different rates, maybe one reversible and one irreversible.

To test whether there was a reversible component to the inactivation, the titration experiment was repeated, first with 0–80 equiv of CPP-115 (Figure S1, Supporting Information), then 0–2000 equiv of CPP-115 (Figure S2, Supporting Information), followed by dialysis. Aliquots removed during dialysis exhibited time-dependent reactivation of GABA-AT over an extended period of time; with increasing equiv of inactivator, less activity returned with maximal return by 24 h (maximal return of activity occurred sooner with less inactivator). It required about 2000 equiv of CPP-115 before the enzyme reactivation was diminished to an insignificant level,

supporting a reversible and irreversible component to the inactivation.

During inactivation of GABA-AT by 2 mM CPP-115, it was found that 66 ± 3 equiv of fluoride ions were released over a 26 h time period; however, enzyme activity was lost within minutes (Figure S3, Supporting Information). This result further supports the notion of two different mechanisms being involved, one reversible and one irreversible, but it does not resolve the question of how many fluoride ions are released per molecule. A single-turnover experiment was carried out to determine the number of fluoride ions per molecule released with each turnover. This experiment is possible because GABA-AT converts substrate to product with concomitant conversion of its PLP to PMP. The reaction cycle cannot restart until α -ketoglutarate binds and converts the PMP back to PLP with concomitant formation of L-glutamic acid. By leaving out the α -ketoglutarate, only one inhibition turnover is possible. Under those conditions, 4.3 ± 0.5 equiv of fluoride ions was detected (Figure S4, Supporting Information); because GABA-AT is a homodimer, two molecules of CPP-115 can be turned over per enzyme dimer. Therefore, 4 equiv of fluoride ion indicates that both fluoride ions in CPP-115 are lost per enzyme turnover, and mechanisms 1, 3, and 4a, which release no fluoride ions

Scheme 5. Second Potential Mechanisms of Inactivation of GABA-AT by CPP-115



during inactivation, and mechanism 4b, which releases one fluoride ion, can be excluded (Table 2).

The cofactor structure after inactivation by CPP-115 was determined using GABA-AT containing [^3H]PLP (Figure S5, Supporting Information). With the aid of two control experiments (Figure S6, Supporting Information), it was found that all of the cofactor was converted to PMP after inactivation (Figure S7, Supporting Information). Therefore, mechanism 4a, which does not release any cofactor and mechanisms 4b, 4c, 5a, and 5b, which require the release of PLP as a cofactor, can be excluded (Table 2).

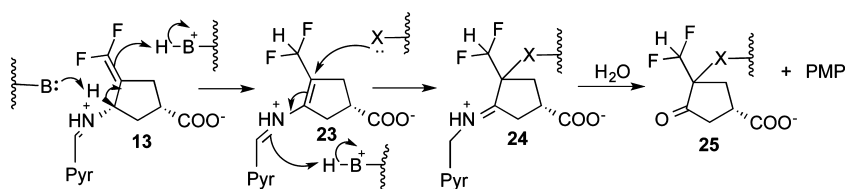
Of the mechanisms considered, only 2a and 2b remain plausible (Scheme 5). Mechanism 2b should produce compounds 20–22. High-resolution LC/MS identified parent ions with m/z 401.0745, 171.0291, and 127.0389 (Figure S8, Supporting Information), which corresponds to 20, 21, and 22, respectively. MS/MS fragmentation produced daughter ions (Figures S9–S11, Supporting Information) consistent with these three products and with mechanism 2b. This mechanism appears to be responsible for the reversible component of the overall inactivation mechanism; mechanism 2a would be expected to account for the irreversible component, so it was imperative to demonstrate covalent attachment to the enzyme (19, Scheme 5) for substantiation.

Mass spectrometry of the intact mass of CPP-115-inactivated GABA-AT was carried out using LC/MS/MS on native enzyme as the negative control and vigabatrin-inactivated GABA-AT as the positive control (Figure S15, Supporting Information). Compared with native enzyme, vigabatrin-inactivated GABA-AT had an added m/z peak of 122 Da, which corresponds to the expected added mass of the covalent adduct previously proposed.¹⁵ CPP-115-inactivated GABA-AT showed no significant peaks corresponding to added mass. In case the potential covalent adduct with CPP-115 was an imine, the inactivated enzyme was reduced with sodium borohydride prior to LC/MS/MS (Figure S16, Supporting Information). Again, no added mass was detected with the CPP-115 inactivated enzyme, but the vigabatrin-inactivated enzyme had the expected added mass. These results were corroborated by results from peptide proteomics (Supporting Information, Figures S13 and S14). Therefore, CPP-115 appears to be inactivating GABA-AT without covalent modification.

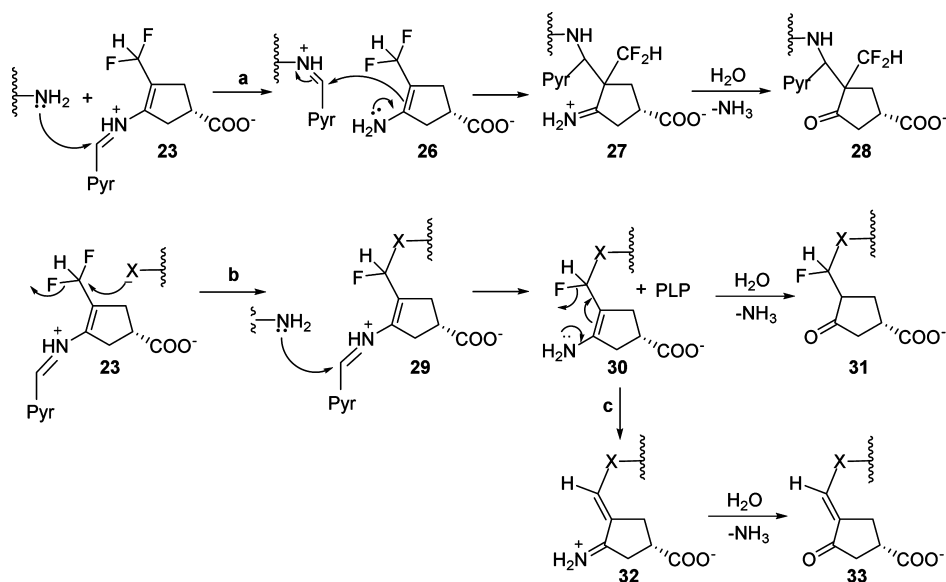
The solution to this dilemma came from the X-ray crystal structure of CPP-115-inactivated pig brain GABA-AT, which revealed that the inactivator was tightly bound to the protein noncovalently as 20 (Figures 3 and 4). The inactivated species binds tightly (stable to dialysis) because of its covalent attachment to the cofactor and by two strong electrostatic interactions between the guanidinium groups of Arg192 and Arg445 and each of the two carboxylate groups of 20. This unexpected phenomenon is the first time that Arg445 has been observed interacting directly with a ligand and to be involved in the inactivation of GABA-AT. On the basis of crystallography of GABA analogues, it is believed that GABA binds in the active site by Schiff base formation with PLP and an electrostatic interaction between the carboxylate of GABA and the guanidinium group of Arg192. Arg445 is sequestered from the active site by an electrostatic interaction with Glu270.²⁵ It has been proposed that this second salt bridge only disassociates during the second half of catalysis, the regeneration of PLP from PMP, to aid in the binding of the second carboxylate of α -ketoglutarate. A network of hydrogen bonds in the active site of GABA-AT connects Glu270 and Arg445 to O3' of the cofactor through the side chain amide of Gln301. Markova et al. proposed that this network may be affected when the cofactor is in its PMP form, which weakens the interaction between Glu270 and Arg445.²⁶ To verify these hypotheses, many research groups have attempted to cocrystallize GABA-AT with ligands such as α -KG or glutamate that may directly show the involvement of this second arginine, but they have not yet been successful.^{25–27}

Our crystal structure of GABA-AT inactivated by CPP-115 (Figure 3) clearly shows for the first time that the salt bridge between Arg445 and Glu270 has been broken, and Glu270 is rotated away from its original position to accommodate a second guanidinium–carboxylate electrostatic interaction between Arg445 and the newly formed carboxylate group on 20

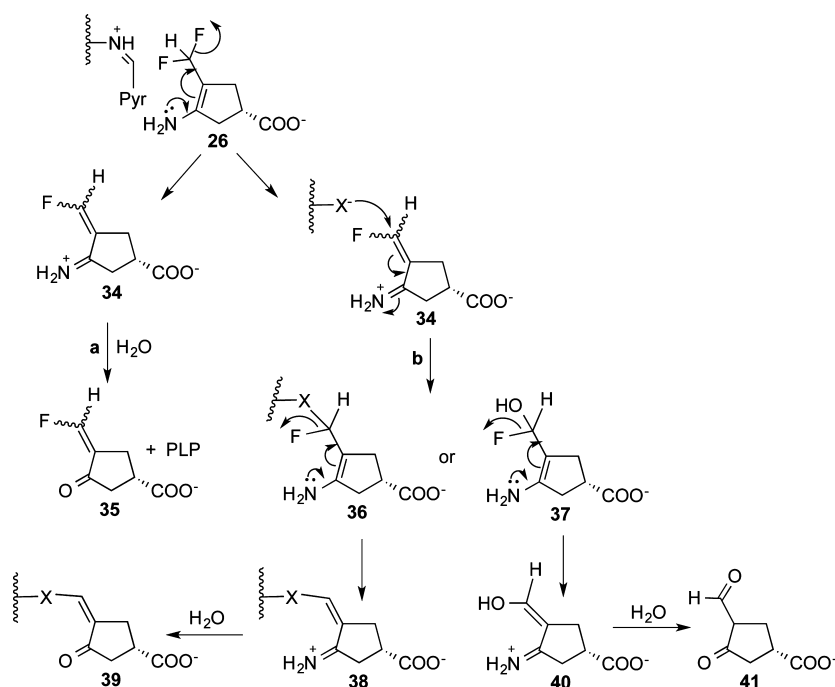
Scheme 6. Third Potential Mechanism of Inactivation of GABA-AT by CPP-115



Scheme 7. Fourth Potential Mechanism of Inactivation of GABA-AT by CPP-115



Scheme 8. Fifth Potential Mechanism of Inactivation of GABA-AT by CPP-115

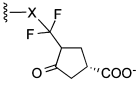
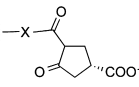
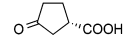
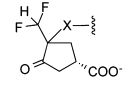
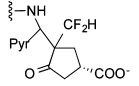
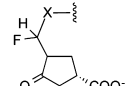
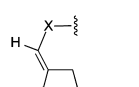
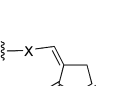
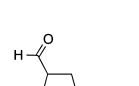


from enzyme-catalyzed hydrolysis of the difluoromethenyl group. The two guanidinium–carboxylate interactions, the hydrophobic interactions of the pyridine ring, and the interactions of the phosphate group contribute to the stabilization of the metabolite for tight binding. Therefore, CPP-115 appears to be, to the best of our knowledge, the first example of a mechanism-based inactivator that leads to a conformational change, forming a tightly bound inhibitor–enzyme complex with a newly exposed residue. Apparently, this conformational change occurs only about once with 2000 molecules of inactivator; the remaining molecules of 20–22 are slowly released as products.

The α,β -unsaturated intermediate (14, Scheme 4) generated during turnover is highly electrophilic, which should have been attacked by the nucleophilic Lys329 residue and form a

covalent adduct, as it does with vigabatrin. Molecular modeling studies of the CPP-115–PLP aldimine were performed to analyze the effect of tautomerization during the inactivation of GABA-AT by CPP-115 (Figure 5). This model demonstrates that the PMP-imine form (orange) of the aldimine generated during enzyme-catalyzed tautomerization shifts the difluoromethenyl group (fluorines are in green) away from Lys329, thereby moving it too far for Michael addition by this lysine residue. Because of the lack of 1,5 steric interactions (both carbons opposite the carboxylate group are sp^2 -hybridized and thus planar), the difluoromethenyl group is able to release strain by moving closer to the carboxylate. As GABA-AT normally catalyzes hydrolysis of the imine formed by tautomerization of GABA, the catalytic machinery is in place for water attack of the Michael acceptor instead. This is

Table 2. Expected Differences in the Various Inactivation Mechanisms

Mechanism	Fluoride release	Cofactor release	Final adduct/ Metabolite released
1	No	PMP	
2a	Yes (2 F ⁻)	PMP	
2b	Yes (2 F ⁻)	PMP	
3	No	PMP	
4a	No	Enzyme bound	
4b	Yes (1 F ⁻)	PLP	
4c	Yes (2 F ⁻)	PLP	
5a	Yes (2 F ⁻)	PLP	
5b	Yes (2 F ⁻)	PLP	

consistent with the obtained crystal structure and explains why the inactivation mechanism did not follow that of vigabatrin and form a covalent adduct.

On the basis of the evidence from fluoride release, cofactor release, metabolites formed, proteomics, and X-ray crystallography, the most consistent mechanism is shown in Scheme 9.

CONCLUSIONS

Although CPP-115 was rationally designed to inactivate GABA-AT via a covalent Michael addition mechanism, the results described here indicate that it inactivates GABA-AT by mechanism-based formation of a metabolite that induces a conformational change and forms a tightly bound complex with the enzyme (Scheme 9). The requirement of about 2000 equiv of CPP-115 for complete inactivation of GABA-AT reflects the number of molecules of product that are released prior to interception by the enzyme in the correct state and conformation that lead to inactivation. Proteomic studies could not reveal a covalent adduct. The crystal structure of CPP-115-inactivated GABA-AT revealed, for the first time, that the Glu270-Arg445 salt bridge in the active site can be disrupted, leading to the formation of a new binding pocket for the inactivator. Our molecular modeling studies indicate a movement of the difluoromethenyl group upon tautomerization, which shifts that group too far from Lys329 for

nucleophilic attack. This leads to enzyme-catalyzed hydrolysis of the PMP-alimine of CPP-115 and either release of products (2000 times) or inducement of a conformational change to give a tightly bound PMP complex stabilized by the exposure of Arg445 and formation of an electrostatic interaction with the newly formed carboxylate of the inactivator. Once metabolite **20** is tightly bound to the enzyme, it is released from the active site very slowly, which accounts for the extended period of time that fluoride ions are released relative to the rate of inhibition of the enzyme. With our results revealing the possibility of additional binding with Arg445, future inactivators may be designed so that the newly formed carboxylate group more closely mimics the second carboxylate group of α -ketoglutarate to encourage less turnover prior to conformational change-induced exposure of Arg445.

EXPERIMENTAL PROCEDURES

Analytical Methods. GABA-AT assays were recorded on a Synergy H1 hybrid multimode microplate reader (Biotek, USA) with transparent 96-well plates (Greiner bio-one, Monroe, NC). Measurements of pH were performed on a Fisher Scientific AP71 pH/mV/°C meter with a pH/ATC electrode. Determinations of fluoride ion concentration were performed on the same meter with a Thermo Scientific 9609BN combination fluoride electrode. Large-scale dialyses were performed with Thermo Scientific Slide-A-Lyzer dialysis cassettes (molecular weight cutoff of 10 kDa) unless otherwise specified. Small-scale dialyses were performed with EMD Chemicals D-Tube Mini dialyzer (molecular weight cutoff of 12–14 kDa). Radioactivity was determined with a Packard TRI-CARB 2100TR liquid scintillation analyzer using PerkinElmer ULTIMA GOLD scintillation fluid. For centrifugations, a DuPont Sorvall RC 5B Plus centrifuge was used with either an SLA-3000 or an SA600 rotor. Eppendorf Minispin plus tubes were used for microcentrifugation. An IEC clinical centrifuge was used for the Penefsky spin method. HPLC analysis was performed with Beckman 125P pumps and a Beckman 166 detector. All of the runs were monitored at 254 nm. The HPLC columns used were Alltech C18 analytical and Econosil 10 μ m columns. Enzyme purification was carried out on a GE Healthcare Life Sciences AKTA FPLC system. The column media used were CM Sepharose Fast Flow for weak cationic exchange mode, DEAE Sepharose Fast Flow for weak anionic exchange mode, and hydroxylapatite (HA) for mixed mode. A prepacked Hiprep Sephacryl S-200 high-resolution column was used for size-exclusion mode. Electrophoresis was carried out on a Bio-Rad Mini-Protein Tetra Cell using a VWR AccuPower Model 300 power supply. LC/MS/MS was performed on Thermo Fisher Q Exactive mass spectrometer. Mass spectrometry of intact mass of GABA-AT was performed on a Velos Orbitrap Elite (ThermoFisher). Crystallographic data were collected on beamline 23 ID-B and 23 ID-D of GM/CA of the Advanced Photon Source (APS) using X-rays of 0.99 Å wavelength and a Rayonix (formerly MAR-USA) 4 × 4 tiled CCD detector. All data were indexed, integrated, and scaled with HKL2000. Data processing statistics are given in Table S1 in Supporting Information.

Reagents. All reagents and materials were purchased from Sigma-Aldrich Co. except the following: Centrifugal filters (molecular weight cutoff value of 10 kDa and 30 kDa) were purchased from EMD Millipore; Dowex 50 and sodium dodecyl sulfate were purchased from Bio-Rad; [³H]sodium borohydride was purchased from American Radiolabeled Chemicals, Inc.; pig brains were a generous gift from the Park Packing Co. (Chicago, IL); all of the buffers and solvents used for FPLC analyses were filtered through GE Healthcare 0.45 μ m nylon membranes. GABase (*Pseudomonas fluorescens*) and succinic semialdehyde were purchased from Sigma-Aldrich.

Enzyme and Assays. GABA-AT (2.65 mg/mL, specific activity 2.1 unit/mg) was purified from pig brain by the procedure described previously.²⁸ Succinic semialdehyde dehydrogenase (SSDH) was obtained from GABase, a commercially available mixture of SSDH and GABA-AT, using a known procedure.²⁴ GABA-AT activity was

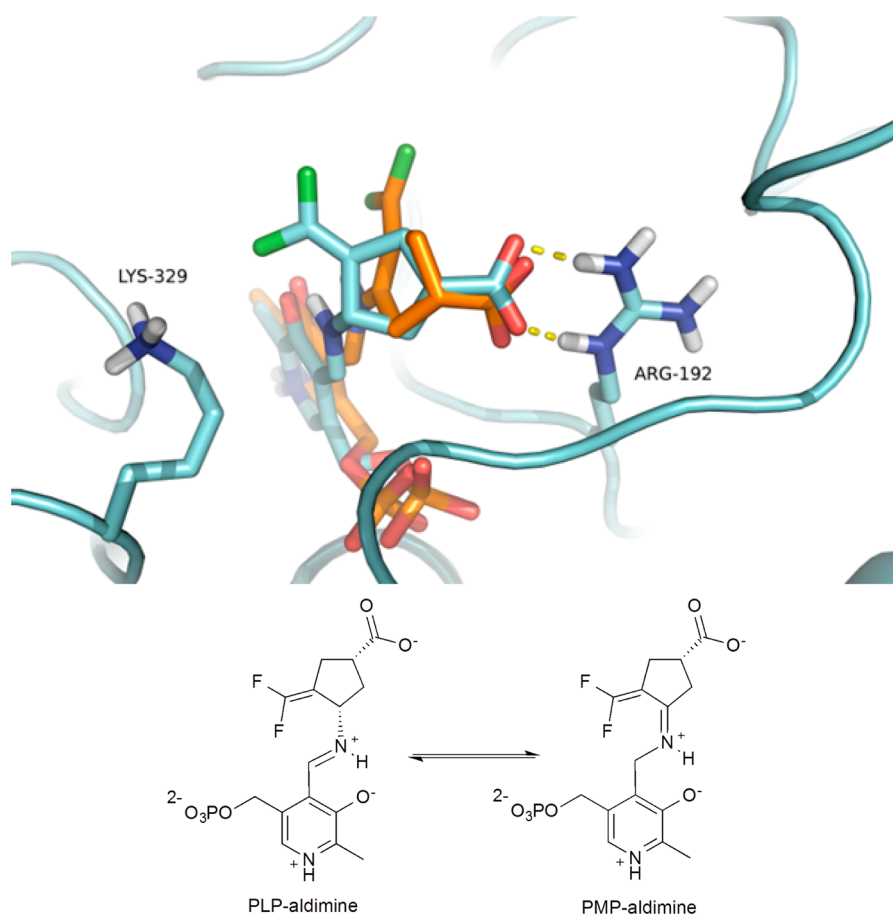


Figure 5. Molecular docking studies of CPP-115-PLP aldimine in PLP-form (cyan) vs CPP-115-PMP-form (orange) in the active site of GABA-AT.

assayed using a published method.²⁹ The final assay solution consisted of 11 mM GABA, 1.1 mM NADP⁺, 5.3 mM α -KG, 2 mM β -mercaptoethanol, and excess SSDH in 50 mM potassium pyrophosphate buffer, pH 8.5. The change in UV absorbance at a wavelength of 340 nm at 25 °C caused by the conversion of NADP⁺ to NADPH is proportional to the GABA-AT activity. All enzyme assays were recorded with a PerkinElmer Lambda 10 UV/vis spectrophotometer.

Syntheses of (1S,3S)-3-Amino-4-difluoromethylene-1-cyclopentanoic Acid (CPP-115). This compound was synthesized according to the procedure published by Pan et al.²⁴

Inhibition of GABA-AT by Various Equivalents of CPP-115. GABA-AT (2 μ g) was incubated with CPP-115 (0, 0.2, 0.4, 0.6, 0.8, 1.0, 1.2, 1.4, 1.6, 1.8, and 4 equiv) at 25 °C in 50 mM potassium pyrophosphate buffer solution, containing 2 mM α -ketoglutarate and 1 mM β -mercaptoethanol. Aliquots (2 μ L) were withdrawn at timed intervals and were added immediately to the assay solution (96 μ L) containing excess SSDH (2 μ L). The reaction rates were monitored at 340 nm.

Inactivation of GABA-AT by CPP-115 and Dialysis of the Inactivated Enzyme. GABA-AT (60 μ L; final concentration 1 μ M) was preincubated for 3 h with various amounts of CPP-115 (0, 1, 1.8, 4, 40, and 80 equiv) in 50 mM pyrophosphate buffer (pH 8.5) containing 0.625 mM α -ketoglutarate, in a total volume of 160 μ L at 25 °C. In another experiment, it was preincubated for 24 h with various amounts of CPP-115 (0, 1, 2, 4, 40, 80, 100, 1000, and 2000 equiv). After preincubation, the enzyme solutions were transferred to D-Tube Mini dialyzers and exhaustively dialyzed against buffer (50 mM pyrophosphate buffer containing 0.1 mM α -ketoglutarate and 0.1 mM PLP, pH 8.5) at 4 °C. The dialysis buffer was exchanged every 4 h, three times. The enzyme activity remaining in each of the solutions was assayed per time interval.

Analysis of Fluoride Ion Release during Inactivation of GABA-AT by CPP-115. GABA-AT (150 μ L) was incubated in 100

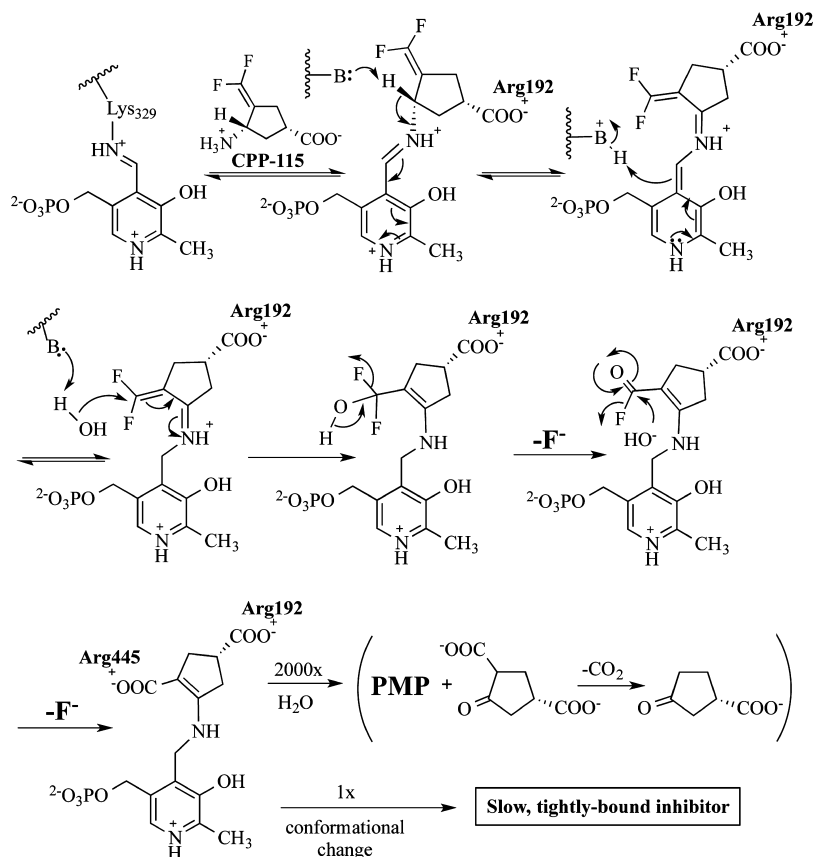
mM potassium pyrophosphate buffer at pH 8.5, containing 2 mM CPP-115 and 2.5 mM α -ketoglutarate in a total volume of 510 μ L. A control lacking GABA-AT was also incubated. The incubation mixture was protected from light and was carried out at room temperature. The experiment was repeated with 2.5 mM PLP supplemented in the incubation mixture.

To construct a standard curve, the relative potential (mV) of sodium fluoride solutions in the range of 1×10^{-6} to 5×10^{-5} M in total ionic strength adjustment buffer (TISAB; made from 5.8 g of sodium chloride and 5.7 mL of acetic acid in 100 mL of water, adjusted to pH 5.2) was measured. The measured potential was plotted against the concentration of sodium fluoride. At different incubation time (1, 2, 5, 7, 17, 24, 27 h), each aliquot was removed from the incubation samples and mixed with TISAB to measure their relative potentials. Using the formula obtained from the standard curve, the mV readings were converted to concentration of fluoride ions in the samples. The readings from the control sample were subtracted from the inactivated sample, and the concentration was divided by the concentration of GABA-AT to obtain the equivalents of fluoride ion released per inactivation event.

Analysis of Fluoride Ion Release during Inactivation of GABA-AT by CPP-115 without α -Ketoglutarate. The similar experiment was run as above but without α -ketoglutarate to test the amount of fluoride released during a one-turnover event. GABA-AT (200 μ L) was incubated in 100 mM potassium pyrophosphate buffer at pH 8.5, containing 2 mM CPP-115 in a total volume of 510 μ L. When there is no α -ketoglutarate in the mixture to regenerate PLP, the reaction stops at one turnover per active site.

Radioactive Labeling of [7-³H]-PLP with Tritiated NaBH₄. Thirty drops of 1 M NaOH were added to 1.8 mL of 0.5 M PLP and cooled to 0 °C in an ice bath. The mixture of sodium borohydride (5.8 mg, 0.15 mmol) and [³H]-sodium borohydride (25 mCi) in 450 μ L of 0.1 M NaOH was added to the PLP solution and stirred for 1 h at 0

Scheme 9. Mechanism of Inactivation of GABA-AT by CPP-115 Most Consistent with Experimental Evidence



°C. After being stirred, 120 μL of concd HCl was added to the solution slowly (became pH 4). To the solution at pH 4, 20 equiv of ground MnO_2 was added, and the mixture was stirred at room temperature for a total of 2 h. The mixture was brought to pH 8 with 1 M NaOH, and the solution was centrifuged. The supernatants were collected and were loaded onto a gel filtration column packed with Bio-Rad AG1-X8 resin (hydroxide form). The mobile phase used was water and 5 M acetic acid (gradient of 90% water to 0% water), flowing at 1.5 mL/min for 300 min. Fractions were collected every 10 mL and tested for its UV absorption and radioactivity. The fractions with desired product were lyophilized. The lyophilized product was redissolved in 100 μL of 1 mM PLP and loaded onto an HPLC with an Econosil C18 column (10 mm \times 250 mm, 10 μm). The mobile phase used was 0.1% aqueous TFA with 5% acetonitrile flowing at 0.5 mL/min for 40 min. Under these conditions, PLP eluted at 15 min. Fractions running with the PLP peak were collected and counted for radioactivity using liquid scintillation counting. The product was collected and lyophilized.

Inactivation of [³H]PLP-Reconstituted GABA-AT by CPP-115. GABA-AT that had been reconstituted with [³H]PLP was incubated at room temperature and protected from light in 100 mM potassium phosphate buffer containing CPP-115 (2 mM), α -ketoglutarate (3 mM), and β -mercaptoethanol (3 mM), in a total volume of 100 μL at pH 7.4. A negative control was run under identical conditions as above, excluding the inactivator. A positive second control was run with 3 mM GABA in the absence of inactivator and α -ketoglutarate. The first control should release the cofactor as PLP, and the second control should release it as PMP. After incubation for 18 h, the activity of GABA-AT was less than 1% of control, and the solutions were adjusted to pH 11 with 1 M KOH and incubated for 1 h. Trifluoroacetic acid (TFA) was added to quench the base and make the solution 10% v/v TFA. The resulting denatured enzyme solution was microcentrifuged for 5 min at 10 000 rpm after standing at room temperature for 10 min. A small amount of white solids was seen at the bottom of the tube. The supernatants were collected individually. To

wash the pellets, 50 μL of 10% TFA was added to each tube, vortexed, and microcentrifuged for another 5 min. This process was repeated three times. The washed pellets were counted for radioactivity. The supernatant and washes were combined and lyophilized. Cofactor analysis was carried out by dissolving the solids obtained from lyophilization with 100 μL of a solution containing 2.5 mM PLP and 2.5 mM PMP as standards and then injecting the samples into the HPLC with an Econosil C18 column (4.6 mm \times 150 mm, 10 μm). The mobile phase used was 0.1% aqueous TFA flowing at 0.5 mL/min for 25 min. Then the flow rate was increased to 1 mL/min from 25 to 30 min, and then a solvent gradient into 95% acetonitrile was run over the next 30 min. Under these conditions, PLP eluted at 15 min and PMP at 8 min. Fractions were collected every minute, and the radioactivity was measured by liquid scintillation counting.

Mass Spectrometric Analysis of Metabolites from Inactivation of GABA-AT with CPP-115. GABA-AT (0.3 nmol) was incubated in 50 mM ammonium bicarbonate buffer (pH 7.4) containing 0.1 mM CPP-115, 1 mM α -ketoglutarate, and 0.1 mM PLP in a total volume of 70 μL at room temperature in the dark for 12 h. A control containing everything except CPP-115 was also incubated. After 12 h, GABA-AT in the inactivated sample was less than 1% active vs control. Formic acid (1 μL) was added to each reaction mixture, and both were centrifuged in a 0.5 mL 30 kDa MWCO centrifuge tube (Millipore) at 14000g for 4 min or until most of the solution had passed through. An additional 20 μL of 50 mM ammonium bicarbonate was added above the filter and centrifuged for 3 min. The flow-through (20 μL) was injected onto a Luna C18(2) column (100 A, 2 \times 150 mm, 5 μm , Phenomenex). A 60 min gradient (Agilent 1100 HPLC, solvent A = 5% acetonitrile and 0.1% formic acid; solvent B = 0.1% formic acid in acetonitrile) was run from 2–80% B over 40 min. The LC was directly connected to a Thermo Fisher Q Exactive mass spectrometer. The top five most abundant ions in negative ion mode were selected for fragmentation using mass normalized collision energies. Commercially available 3-oxo-1-cyclopentanecarboxylic acid (Sigma) was injected as a standard for comparison.

Intact Mass Spectrometry of GABA-AT. Three reaction samples were prepared as described previously with only GABA-AT, including vigabatrin, or CPP-115.³⁰ After incubation with or without inhibitors, half of each reaction mixture was reduced with 15 mM sodium cyanoborohydride for 1 h. Both reduced and nonreduced samples were buffer exchanged into 50 mM ammonium acetate using 30 kDa MWCO filters (Millipore). Nano-LC/MS/MS runs were done on a 75 μm ID \times 10 cm Kinetex C8 (Phenomenex) column connected to an autosampler (Dionex Ultimate 3000 RSLCnano system) and a Velos Elite Orbitrap (ThermoFisher) mass spectrometer. Results were deconvoluted using ProMass Deconvolution software (Thermo Scientific).

Enzyme Crystallization. Before crystallization, GABA-AT and CPP-115-inactivated GABA-AT were exchanged into a buffer that contained 40 mM sodium acetate (pH 5.5). After the initial crystallization screening and optimization, the proteins were crystallized via the hanging drop method. Hanging drops were prepared by mixing 1 μL of 12 mg/mL native GABA-AT protein solution and 1 μL of the reservoir solution, containing 0.1 M ammonium acetate, 0.1 M bis-Tris (pH 5.5), and 17% w/v PEG 10 000. Crystals appeared within 24 h at 20 $^{\circ}\text{C}$ and grew for 5–6 days before harvesting. Crystals with good morphology and large sizes were transferred to cryoprotecting conditions, which contain 20% glycerol in addition to the original composition of the reservoir solution, before being frozen in liquid nitrogen. The same method of crystallization was applied for CPP-115-inactivated GABA-AT; however, before freezing in liquid nitrogen, the inactivated crystals were transferred to a cryoprotecting solution that contained 20% glycerol and 2 mM CPP-115, in addition to the compounds of the reservoir solution. Crystallographic data were collected on beamlines 23ID-B and 23ID-D of GM/CA@APS of the Advanced Photon Source (APS) using X-rays of 0.99 \AA wavelength and Rayonix (formerly MAR-USA) 4 \times 4 tiled CCD detector with a 300 mm² sensitive area. All data were indexed, integrated, and scaled with HKL2000. Data collection and processing statistics are given in Table S1 (Supporting Information).

Phasing, Model Building, and Refinement. Molecular replacement for the native GABA-AT was carried out using the program Phaser³¹ from CCP4³² software suite, using the previously reported coordinates of GABA-AT from pig liver (PDB ID: IOHV) as the starting search model. The initial R_{free} and R factor of the correct solution were 0.1904 and 0.1934, respectively. The rigid body refinement was followed by restrained refinement using Refmac5.³³ Manual adjustment and modification of the structure based on electron density maps were performed using the program Coot.³⁴ The R_{free} and R factor values of the final model were 0.1513 and 0.1766, respectively.

The data sets from the inactivated GABA-AT crystals were isomorphous to those of native GABA-AT. Therefore, rigid body refinement could be used directly, placing the previously refined native GABA-AT model into the asymmetric unit of inactivated GABA-AT crystals. Model building and refinements of the inactivated structures were carried out following the same protocol as the native structure. There were no ligand coordinates included in the refinement until the refinement converged. Without ligands built in, the $F_o - F_c$ map shows a well-defined electron density supporting the existence of the bound ligand.

The structure of the inactivator was made in the program ChemDraw generating a “Mol” file as the output. This output ligand structure was then regularized and its chemical restraints were generated in the program JLigand.³⁵ Using Coot, the inactivator was manually fit to the residual electron density in the difference ($F_o - F_c$) map. The complex structure with the ligand bound was further refined in Refmac5. The R_{free} and R factor for the inactivated structure were 0.1575 and 0.1872, respectively.

Molecular Modeling. All renderings were performed in PyMol.³⁶ Computer simulations were carried out as previously described.³⁷ In essence, the ligands (including the cofactor) were docked into the active site of the prepared protein using Autodock 4.2,³⁸ with Lys329 being flexible. The best docked structures were then refined by molecular mechanics, using GROMACS 4.5.³⁹ The sequence utilized

started with energy minimization, continued with molecular dynamics (4 ns), and had a final energy minimization step. The final structures were used for evaluation.

■ ASSOCIATED CONTENT

📄 Supporting Information

Reactivation results of GABA-AT after inactivation; fluoride ion release results; cofactor release results; high resolution mass spectra; mass fragmentation data of metabolites 20–22; middle down peptide proteomics results, omit map for inactivated enzyme, crystallography data collection, processing statistics. This material is available free of charge via the Internet at <http://pubs.acs.org>.

■ AUTHOR INFORMATION

Corresponding Author

*Agman@chem.northwestern.edu

Present Addresses

[†]Molecular Recognition Research Center, Korea Institute of Science and Technology (KIST), Seoul, Korea.

[‡]Department of Chemistry, Salisbury University, Salisbury, MD 21801.

Notes

The authors declare no competing financial interest.

■ ACKNOWLEDGMENTS

The authors are grateful to the National Institutes of Health for financial support (grants GM066132 and DA030604 to R.B.S.; GM067725 to N.L.K.; contracts ACB-12002 and AGM-12006 to R.S. This research used resources of the Advanced Photon Source, a U.S. Department of Energy (DOE) Office of Science User Facility operated for the DOE Office of Science by Argonne National Laboratory under Contract No. DE-AC02-06CH11357.).

■ REFERENCES

- (1) Krnjevic, K. *Physiol. Rev.* **1974**, *54*, 418–540.
- (2) Karlsson, A.; Fonnum, F.; Malthe-Sørensen, D. *J. Biochem. Pharmacol.* **1974**, *23*, 3053–3061.
- (3) Davies, P. *Brain Res.* **1979**, *171*, 319–327.
- (4) Perry, T. L.; Hansen, S.; Tischler, B.; Richards, F. M.; Sokol, M. *N. Engl. J. Med.* **1973**, *289*, 395–398.
- (5) Maker, H. S.; Weiss, C.; Weissbarth, S.; Silides, D. J.; Whetsell, W. *Ann. Neurol.* **1981**, *10*, 377–383.
- (6) Rinne, U. K.; Laaksonen, H.; Riekkinen, P.; Sonninen, V. *Eur. Neurol.* **1974**, *12*, 13–19.
- (7) Dewey, S. L.; Morgan, A. E.; Ashby, C. R., Jr.; Horan, B.; Kushner, S. A.; Logan, J.; Volkow, N. D.; Fowler, J. S.; Gardner, E. L.; Brodie, J. D. *Synapse* **1998**, *30*, 119–129.
- (8) Karila, L.; Gorelick, D.; Weinstein, A.; Noble, F.; Benyamina, A.; Coscas, S.; Blecha, L.; Lowenstein, W.; Martinot, J. L.; Reynaud, M.; Lepine, J. P. *Int. J. Neuropsychopharmacol.* **2008**, *11*, 425–438.
- (9) Hearl, W. G.; Churchich, J. E. *J. Biol. Chem.* **1984**, *259*, 11459–11463.
- (10) Baxter, C. F.; Roberts, E. *J. Biol. Chem.* **1958**, *233*, 1135–1139.
- (11) Purpura, D. P.; Girando, M.; Smith, T. A.; Callan, D. A.; Groundfest, J. *J. Neurochem.* **1959**, *3*, 238–268.
- (12) Hammond, E. J.; Wilder, B. J. *Gen Pharmacol* **1985**, *16*, 441–447.
- (13) (a) Silverman, R. B. *Methods Enzymol.* **1995**, *249*, 240–283. (b) Silverman, R. B. *Mechanism-Based Enzyme Inactivation: Chemistry and Enzymology*; CRC Press: Boca Raton, FL, 1988; Vols. I and II.
- (14) Silverman, R. B. *The organic chemistry of enzyme-catalyzed reactions*; Academic Press: San Diego, CA, 2000.

- (15) Lippert, B.; Metcalf, B. W.; Jung, M. J.; Casara, P. *Eur. J. Biochem.* **1977**, *74*, 441–445.
- (16) Nanavati, S. M.; Silverman, R. B. *J. Am. Chem. Soc.* **1991**, *113*, 9341–9349.
- (17) Storici, P.; De Biase, D.; Bossa, F.; Bruno, S.; Mozzarelli, A.; Peneff, C.; Silverman, R. B.; Schirmer, T. *J. Biol. Chem.* **2004**, *279* (1), 363–373.
- (18) Storici, P.; Capitani, G.; De Biase, D.; Moser, M.; John, R. A.; Jansonius, J. N.; Schirmer, T. *Biochemistry* **1999**, *38*, 8628–8634.
- (19) (a) Choi, S.; Storici, P.; Schirmer, T.; Silverman, R. B. *J. Am. Chem. Soc.* **2002**, *124*, 1620–1624. (b) Choi, S.; Silverman, R. B. *J. Med. Chem.* **2002**, *45*, 4531–4539.
- (20) Pan, Y.; Qiu, J.; Silverman, R. B. *J. Med. Chem.* **2003**, *46*, 5292–5293.
- (21) Silverman, R. B. *J. Med. Chem.* **2012**, *55*, 567–575.
- (22) (a) Andrić, P.; Meyer, A. S.; Jensen, P. A.; Dam-Johansen, K. *Biotechnol. Adv.* **2010**, *28* (3), 308–324. (b) Frieden, E.; Walter, C. *Nature* **1963**, *198* (4883), 834–837.
- (23) Pan, Y. Design, synthesis and mechanistic studies of γ -aminobutyric acid aminotransferase inhibitors. Ph.D. Dissertation, Northwestern University, Evanston, IL, June 2004.
- (24) Silverman, R. B.; Bichler, K. A.; Leon, A. J. *J. Am. Chem. Soc.* **1996**, *118* (6), 1241–1252.
- (25) Liu, W.; Peterson, P. E.; Carter, R. J.; Zhou, X.; Langston, J. A.; Fisher, A. J.; Toney, M. D. *Biochemistry* **2004**, *43* (34), 10896–10905.
- (26) Markova, M.; Peneff, C.; Hewlins, M. J. E.; Schirmer, T.; John, R. A. *J. Biol. Chem.* **2005**, *280* (43), 36409–36416.
- (27) Storici, P.; Capitani, G.; Muller, R.; Schirmer, T.; Jansonius, J. N. *J. Mol. Biol.* **1999**, *285* (1), 297–309.
- (28) Silverman, R. B.; Levy, M. A. *J. Biol. Chem.* **1981**, *256*, 11565–11568.
- (29) Scott, E. M.; Jakoby, W. B. *J. Biol. Chem.* **1959**, *234*, 932–936.
- (30) Burke, J. R.; Silverman, R. B. *J. Am. Chem. Soc.* **1991**, *113* (24), 9329–9340.
- (31) McCoy, A. J.; Grosse-Kunstleve, R. W.; Adams, P. D.; Winn, M. D.; Storoni, L. C.; Read, R. J. *J. Appl. Crystallogr.* **2007**, *40*, 658.
- (32) Collaborative Computational Project, N. *Acta Crystallogr., Sect. D: Biol. Crystallogr.* **1994**, *50*, 760.
- (33) Murshudov, G. N.; Vagin, A.; Dodson, J. *Acta Crystallogr., Sect. D: Biol. Crystallogr.* **1997**, *53*, 240.
- (34) Emsley, P.; Cowtan, K. *Acta Crystallogr., Sect. D: Biol. Crystallogr.* **2004**, *60*, 2126.
- (35) Lebedev, A. A.; Young, P.; Isupov, M. N.; Moroz, O. V.; Vagin, A. A.; Murshudov, G. N. *Acta Crystallogr., Sect. D: Biol. Crystallogr.* **2012**, *68*, 431.
- (36) The PyMOL Molecular Graphics System, Version 1.5.0.4 Schrödinger, LLC.
- (37) Juncosa, J. I.; Groves, A. P.; Xia, G.; Silverman, R. B. *Bioorg. Med. Chem.* **2013**, *21*, 903–911.
- (38) Morris, G. M.; Huey, R.; Lindstrom, W.; Sanner, M. F.; Belew, R. K.; Goodsell, D. S.; Olson, A. J. *J. Comput. Chem.* **2009**, *16*, 2785–2791.
- (39) Pronk, S.; Páll, S.; Schulz, R.; Larsson, P.; Bjelkmar, P.; Apostolov, R.; Shirts, M. R.; Smith, J. C.; Kasson, P. M.; van der Spoel, D.; Hess, B.; Lindahl, E. *Bioinformatics* **2013**, *29* (7), 845–854.